

**FEDSM2003-45321**

## CAVITATION IN ICE-MILLING WITH A PODDED PROPULSOR

**Mehmet Atlar, Ika Prasetyawan, Wasis Dwi Aryawan and Dazheng Wang**  
School of Marine Science and Technology  
Newcastle University, Newcastle upon Tyne, United Kingdom

**Noriyuki Sasaki**  
Sumitomo Heavy Industries Ltd., Japan

### ABSTRACT

Some experimental evidence of cavitation and effect of other parameters, which influence the performance of an ice-class podded propulsor in blockage and milling condition, are presented for the first time. Conducting ice-milling tests in cavitation tunnels is extremely rare due to complexity of the tests as well as the neglected effect of cavitation. The paper describes the details of a novel test set up and preliminary results to demonstrate the importance of the cavitation and presents a proposal how to consider this effect in the design of an ice-class propeller.

**Keywords:** Experimental Cavitation, Ice-Milling, Podded Propulsor.

### INTRODUCTION

Propellers operating in arctic conditions are subjected to complex interaction with surrounding ice floes and ridges. The resulting propeller-ice interaction phenomenon can be investigated in three simplified stages that are “impact”, “blockage” and “milling”. The milling is the final stage where the propeller crushes the ice in the vicinity of the propeller disk forming a recess, causing numerous cavitations and loading phenomenon. It is the most complex and poorly understood stage requiring further research, in particular experimental investigation.

During the milling process, the propellers will experience change in loadings (i.e. thrust and torque) due to mechanical contact of the blades with ice and change in hydrodynamics of the blades operating in ice recess. The latter component is due to the proximity effect which induces a high velocity water flow through the small gap between the propeller and ice block which leads to an increased lift force on the blades. The milling process also needs to extrude crushed ice from the damaged

zone, which is ejected at high speed on the back of the propeller generating additional lift on the blades.

Whether the propeller is operating in blockage condition, where a section of ice restricts flow to the propeller changing the flow pattern without any mechanical contact, or in milling condition, it will suffer from numerous cavitation effects, particularly from severe cloud cavitation, as reported in the open literature e.g. [1,2]. Doucet et al [2] performed tests with a 200mm model of propeller of Canadian R-Class ice-breakers behind and inside the recess of a simulated ice blockage at IMD cavitation tunnel, including a set of erosion tests. For this particular model both vortex and severe cloud cavitation were present and erosion resulted even at atmospheric pressure. Later on, the same propeller was tested in the Emerson Cavitation Tunnel in milling conditions by Minchev et al. [e.g. 3, 4]. Based upon the test results it is concluded that, during the milling and low cavitation numbers representing the full-scale conditions, the main reason for a torque increase is the contact loads, whereas the reason for the thrust decrease is the severe cloud cavitation, which occurs when the propeller blades operate in the ice recess. These tests, for the first time, provided evidence on the dominating effect of cavitation, which should be investigated systematically and taken into account in the design of ice class propellers.

Cavitation related problems are a potential danger for any type of propeller operating in ice. The recent introduction of azimuthing podded drives on arctic vessels has revolutionized the arctic transport technology to optimize the overall transport efficiency of arctic vessels as reported by Backlund and Matsuda e.g. [5]. This is achieved by taking advantage of the azimuthing feature of the electric podded drives which can provide an arctic vessel with a double acting role. The aft end of such vessel is optimized for ice-breaking and the vessel operates astern in ice-breaking mode while the bow is optimized for normal open water and going ahead condition

without any compromise in the powering that can result in significant reduction in ice resistance (up to 50%).

Sumitomo Heavy Industries (SHI) Ltd. recently built and launched two ice class Aframax Double Acting Tankers (DAT) of 106,000 DWT, which are equipped by a single Azipod unit for each with a 16 MW pulling power and 7.8 diameter stainless steel propeller. The details of the hydrodynamic design of these vessels and comprehensive model tests performed in conventional and ice-tanks have been reported by Sasaki et al [e.g. 6]. When these tankers operate in ice, particularly in the ice breaking astern mode -also known as DAT mode- the pulling propeller in the front will be subjected to the contact with the ice floes and ridges at heavily loaded conditions. The fully azimuthing propeller in heavy ridges will be actively shaving and helping to breaking up the ridge ahead of the ship hull, and by optimum use of the propeller, the contact between the ship and the surrounding ice will be kept to a minimum. Under these circumstances the effect of the cavitation during the milling will be an essential factor for the performance and design of these types of propulsors.

Within the framework of the above background, a set of exploratory cavitation tunnel tests was performed in the Emerson Cavitation Tunnel to investigate the ice-milling phenomena using the 1/30<sup>th</sup> scale model of the Sumitomo DAT propulsor in the bollard pull and astern (or DAT) conditions as reported by Atlar et al [8] in details. The main objectives of these tests are to provide experimental evidence on cavitation and other parameters affecting the performance of a podded propulsor in blockage and, particularly, in milling condition which are non-existent. In complementing the cavitation tests, further experiments were carried out to investigate effect of the pod housing on the propeller performance as well as the flow field measurements between the ice-block and propulsor using a two dimensional Laser Doppler Velocimetry (LDV) system.

## NOMENCLATURE

- D = Diameter of model propeller
- J = Advance coefficient
- $K_T$  = Thrust coefficient
- $K_Q$  = Torque coefficient
- P = Pitch
- $P_0$  = Atmospheric pressure
- $P_v$  = Vapor pressure
- R = Propeller radius
- Re = Reynolds number
- $\eta_o$  = Open water efficiency
- $\rho$  = Tunnel water mass density = 1005.9 Kg/m<sup>3</sup>
- $\sigma$  = cavitation number based on rate of rotation
- n = Model propeller rate of rotation

## TEST EQUIPMENT AND FACILITIES

### Cavitation Tunnel and Its Instrumentations

All experiments have been conducted in the Emerson Cavitation Tunnel facilities at the University of Newcastle upon Tyne, which have basic particulars as in Table 1, while further details can be found in e.g. [9, 10]. The tunnel is equipped with the LabVIEW data acquisition software.

The present tests used a Kempf & Remmers H33 dynamometer to measure model propeller thrust and torque, with a special arrangement for pod housing as shown in Fig 3. The dynamometer's load measuring capacities are  $\pm 2943$  N of thrust and  $\pm 147$  Nm of torque at a maximum shaft speed of 4000 rpm.

**Table 1 Description of the cavitation tunnel**

Description	Vertical, closed circulating
Test section size (LxBxT)	3.10x1.22x0.81 m
Contraction ratio	4.271
Maximum velocity	15.5 knots (8 m/s)
Absolute pressure range	7.6 kN/m <sup>2</sup> to 106 kN/m <sup>2</sup>

The Emerson Cavitation Tunnel is also equipped with the Laser Doppler Velocimetry (LDV) system, i.e. a two-dimensional fiber-optic, back-scattering mode DANTEC system combined with PDA (Phase Doppler Anemometry) facility that can measure particle size characteristic of the flow as well as velocities. Two components of the flow in a plane can be measured approaching with four-beam laser from one direction at a time. In the present test set-up, the measurements were taken from the bottom window of the tunnel measuring section.

### Model Pod Propulsor

Based upon the full-scale drawings, the model was manufactured to a scale of 1/30<sup>th</sup> of the full scale puller type propulsor of DAT. Its propeller was made of hydronalium PA20 and anodized. The pod body, strut and fin were made from hard plastic and painted. The main details of model and full scale of the podded propulsors are given in Table 2.

**Table 2 Particulars of the podded propulsor**

	Model (mm)	Full scale (mm)
Diameter (D)	250	7800
Number of blades	4	
Direction of rotation	right	
P/D at 0.7R	0.6923	
Blade area ratio	0.54	
Rake	0	
Max. diameter of pod	106.7	3200
Span of strut	131.7	3950
Chord of strut	220.7	6620
Max. thickness of strut	51.3	1540

### Ice Model

In the previous ice milling tests conducted in the Emerson Cavitation Tunnel [3], numbers of different model ice material, including real ice, was considered. Taking into account the restriction imposed by the cavitation tunnel equipment and other factors, a Styrofoam, with a compressive strength of approx. 170 kPa, was selected. Using this material, small model ice blocks were made in 200 mm x 145mm x 60 mm size to fit into the ice-feeding mechanism as shown in Figure 1. Strength characteristics of the foam material for the compression and tension were measured in laboratory and typical result for the compression is shown in Figure 2.



Figure 1 Styrofoam model ice-block

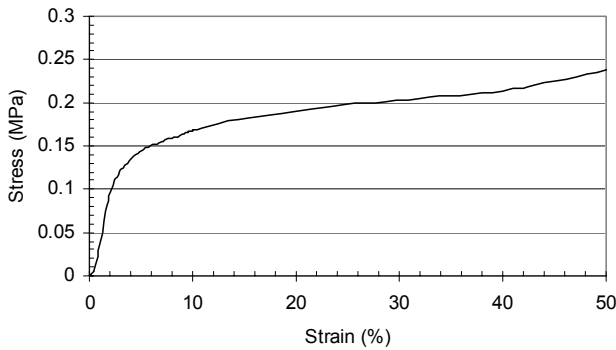


Figure 2 Compressive strength of the ice-block model

### Ice Feeding Mechanism

A hydraulic milling mechanism for simulating milling action was designed and manufactured to handle high suction power, generated by propeller model, and enable high feeding speed of the ice block model. The system was attached on the tunnel lid and covered with GRP streamlined casing to provide a wake flow as uniform as possible on the way of propeller. An ASM (type WS10-1250-PMU-L10) linear position sensor was also installed on the milling mechanism to record ice block model position as well as to drive block speed. The detail of ice feeding mechanism and its arrangement with respect to model pod propulsor is shown in Figure 3.



Figure 3 Ice milling mechanisms and model pod propulsor

## TEST PROGRAM

### Test Conditions

The milling tests were performed at corresponding to full scale operational conditions as follows: (1) Milling at bollard pull condition at 75 RPM, giving  $J = 0$ , (2) Milling at astern condition (DAT mode) at 5 knots and 75 RPM, giving  $J = 0.26$ . Using the shaft rotational speed based cavitation number, defined as:  $\sigma = (P_0 - P_v) / (0.5 \rho n^2 D^2)$ , the corresponding cavitation number was calculated (i.e.  $\sigma = 4.1$ ) and fixed throughout the course of the tests. During the tests, the dissolved oxygen content of the tunnel water solution was measured and kept at 30% - 35% level.

### Test Procedure

Two groups of main tests were conducted, namely: cavitation observations in blockage and ice-milling tests. In addition, open water tests for the model propeller and flow investigation using the LDV were performed prior to these main tests.

The open water tests were performed without the ice milling mechanism and therefore the propulsor was operating in uniform flow of the tunnel. The main purpose of these tests is to verify the reference performance of the propeller (i.e. thrust, torque and efficiency) as well as to quantify the effect of the pod housing on the propeller's performance alone. Therefore, the thrust and torque on the propeller were measured with and without the pod housing at a range of advance coefficient ( $J$ ) values varying between 0.0 (bollard pull condition) and 0.75. The measurements were taken at atmospheric condition at water speeds up to a maximum of 4 m/s and the rotation rate of the shaft was changed incrementally to cover the above range of the advance coefficients. The open water tests were conducted at Reynolds number  $Re > 1 \times 10^6$  to minimise the scaling errors. The flow investigation was carried out by using the LDV. This investigation is intended to gain insight on the nature of flow field behind and between the ice-block and the pod propulsor. Therefore, the axial component of the flow velocities was measured using the LDV corresponding to the earlier selected operational condition (i.e.  $J=0$  and  $J=0.26$ ).

The cavitation observations in blockage were performed to investigate the effect of blockage of the ice-block on the propeller cavitation performance. During these tests, the maximum distance between the ice block and propeller tip was 155 mm (0.62D) and assigned as "Far-Block" distance. The ice block model was then gradually pushed towards the propulsor and stop at the half of the far block distance, which was assigned as "Half-Block" distance. The block was finally stopped at a position just before making mechanical contact with the propeller. This last position was assigned as "Close Block" distance. During these tests no milling was carried out since the objective was to investigate and illustrate the change in the nature and extent of cavitation as the distance between the ice block and propeller is changed. These tests were carried out at the earlier specified operational conditions (i.e.  $J=0$  and  $J=0.26$ ) and 1.5 mm/s of ice-block speed. The associated still photograph and video film were taken to illustrate the nature of cavitation.

The main objectives of the ice milling tests were to provide evidence of cavitation and data during ice-milling phenomena, particularly on cavitation, which cannot be investigated in a normal ice tank. These tests were performed at the earlier described operational conditions (i.e.  $J=0$  and  $J=0.26$ ) corresponding to the bollard pull and DAT mode at  $\sigma = 4.1$ . In order to explore the effect of different block speed and depth of propeller cut in ice-block, two different values for each parameter are selected. A summary of the testing conditions for the ice-milling is given in Table 3 as a test matrix

**Table 3 Matrix of ice milling experiments**

J	Block Speed (mm/s)	Depth of Cut (DOC)
0	1.5	0.2D
		0.1D
	15	0.2D
0.26	1.5	0.2D
		0.1D
	15	0.2D

During the ice-milling tests two different procedures were followed in feeding the ice block, namely: “Continuous” type feeding, and “Stop and go” type feeding. In the continuous feeding, the block was fed towards the propulsor at constant speed without any interruption until the maximum cutting length was reached (i.e. front end of the ice-block to contact with the leading edge of the strut). After a few seconds, the milling process was stopped and the block then was pulled back at a constant speed inside the sliding mechanism. The main objective of the continuous feeding was the measurements of the thrust and torque values without any interruption. In the “stop and go” type of feeding, the main objective was also to observe the cavitation at certain positions of the block. Therefore, the block stopped at the following positions: (1) halfway distant between the tip and block initial position, (2) block just about to touch to blade leading edge, (3) propeller tip flushed with block edge, (4) at the full stroke of the sliding distances, (5) half way in the ice recess. These stop positions provide opportunity to take some photos and videos as well as to make observations and measurements in different stages of the milling.

## TEST RESULTS AND DISCUSSION

### Open Water Diagram of the Model Propeller

Before the milling tests, the model propeller was tested in open water condition and at atmospheric pressure. The propeller thrust and torque was measured for a range of advance coefficient with and without the presence of the pod housing. The values of thrust and torque have been converted into coefficients and values of advance coefficients have also been corrected for tunnel wall effects. The test details and set up may be found in [7].

In order to provide information about the effect of the pod on the propeller’s performance, curves of  $K_T$ ,  $10K_Q$  and  $\eta_o$  (efficiency) to a base of corrected  $J$  without and with the pod housing are given in Figure 4.

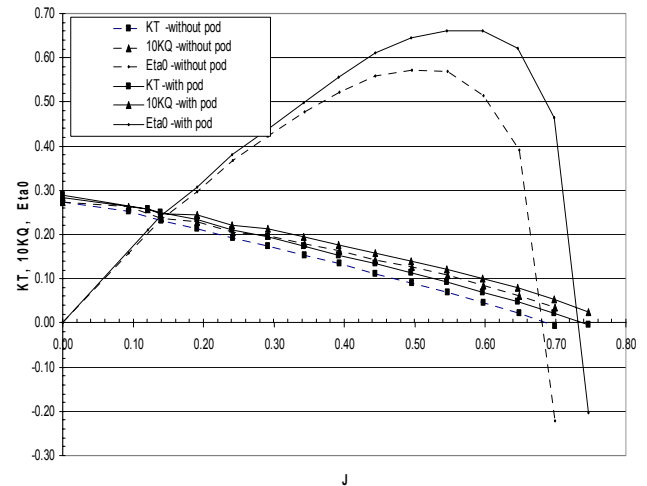


**Figure 4 Comparison of open water diagram with and without pod housing**

As one can see from Figure 4, the thrust and torque coefficients ( $K_T$  and  $K_Q$ ) of the propeller increase due to the presence of the pod housing, leading to a gain in efficiency, except at the very small region of  $J < 0.1$ , where there is a cross-over between  $K_T$  and  $10K_Q$  curves towards  $J=0$ . By considering the design operation condition of the vessel (i.e.  $V_s = 15.2$  knots and  $N = 105$  rpm), the corresponding advance coefficient is  $J = 0.572$ . At this condition, the increase in  $K_T$ ,  $10K_Q$  and  $\eta_o$  due to presence of the pod is 33%, 16% and 22% respectively.

The bollard pull  $K_T$  and  $10K_Q$  values measured in the cavitation tunnel differed from the values measured in the Sumitomo towing tank by less than 1% for the propeller in isolation and less than 2.8% when the propeller is in front of the pod.

Although the above tests were performed at the atmospheric condition, it was observed that the cavitation inception with the pod housing was occurred at lower rpm than without the pod housing.

### Flow Field

In order to gain insight on the nature of the flow to the propeller and to help in understanding interaction between propeller and blocking ice, flow measurements were made using a 2-D LDV at bollard pull and  $J=0.26$ . However, only flow measurements at bollard pull condition are presented here, whilst complete results can be found in [8].

The axial component of the flow velocities were taken in front of the propeller without and with the presence of ice milling mechanism, as shown in Figure 5 and Figure 6, respectively.

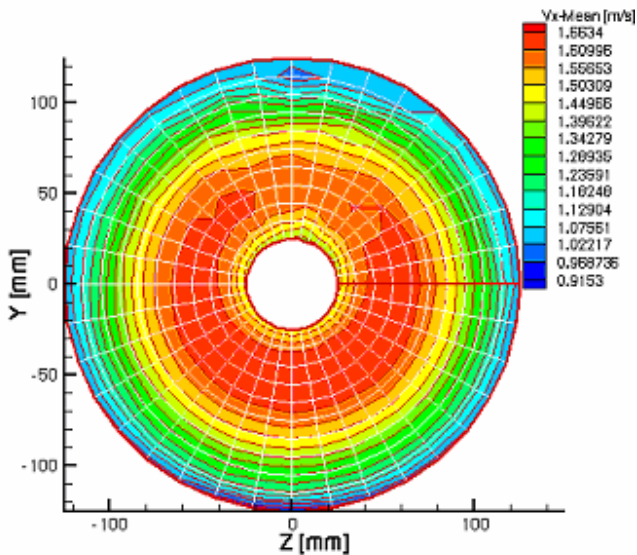


Figure 5 Axial velocity distribution without ice-block at bollard condition

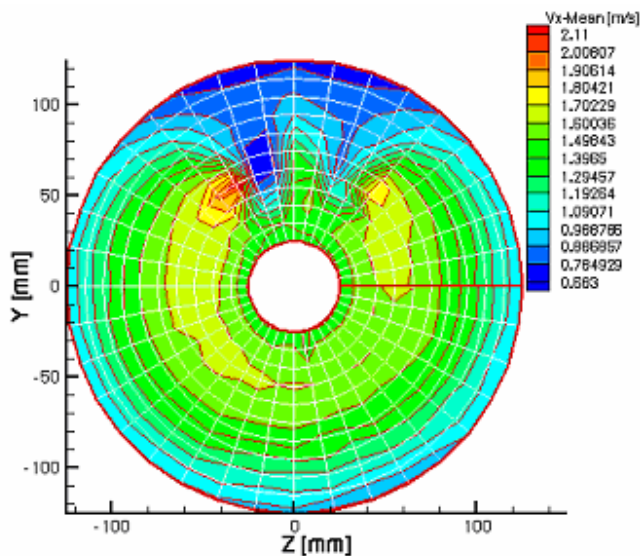


Figure 6 Axial velocity distribution with ice-block at bollard condition

In the bollard pull condition, looking at Figure 5, the axial induced velocity distribution of the propeller without the effect of ice-block is quite uniform and increasing from tip to root. As shown in Figure 6, the introduction of the ice-block reduces the magnitude of the induced axial flow velocities towards the propeller at about maximum of 38% in the wake shadow region. The induced velocity field over the disk and outside the wake shadow is also slowed down.

#### Cavitation Observations in Blockage Condition

As stated earlier, preliminary cavitation tests were conducted at two operational conditions  $J=0$  and  $J=0.26$  at  $\sigma = 4.1$  in blockage condition. Figure 7 shows a global appearance of the cavitating podded propeller behind the milling mechanism at bollard pull ( $J=0$ ) condition while Figure 8 displays similar appearance at DAT condition ( $J=0.26$ ).



Figure 7 Cavitation at podded propulsor at bollard pull condition



Figure 8 Cavitation at podded propulsor at DAT mode ( $J=0.26$ )

As one can see from Figure 7 and Figure 8, during the cavitation tests in blockage condition, while the ice-block is at the farthest distance away from the propeller tip ( $0.3D$ ), a well developed strong tip vortex cavitation emanating from all four blades and striking the pod housing in downstream can be observed.

Figure 9 and Figure 10, on the other hand, illustrates the zoomed appearance of the propeller blade at the top dead centre position for  $J=0$  and  $J=0.26$ , respectively, for three different positions of the model ice block.

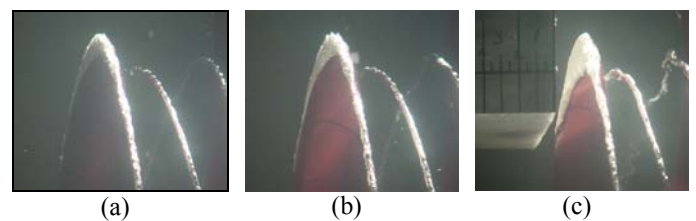


Figure 9 Cavitation observation (zoomed) at bollard pull condition: (a) far block, (b) half block and (c) close block

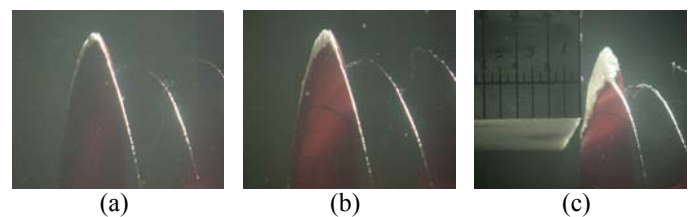


Figure 10 Cavitation observation (zoomed) at DAT mode: (a) far block, (b) half block and (c) close block

As shown in Figure 9 (a), a close look into the bollard pull condition indicates that the strong tip vortex cavitation is also incorporated with a slight sheet cavitation at the blade tip regions approximately less than 0.95R. As the block approaches towards the propeller, which can be shown in Figure 9 (b) and Figure 9 (c), the extent of the sheet vortex cavitation in the wake shadow of ice-block increases to 0.9R and takes a glassy appearance with increased intensity. In downstream, wherever the tip vortex strips hit the pod housing, the vortices burst into cloud cavitation at both sides of the strut.

Figure 10 (a) shows a tip vortex cavitation in the DAT mode that extends in the down stream striking the pod housing. However, as the block approaches to the propeller, which is illustrated by Figure 10 (b) and Figure 10 (c), tip vortex cavitation transforms to sheet cavitation extending to 0.9R at maximum that is similar to the bollard pull condition. However, the intensity of the tip vortex cavitation is at much lesser extend than in the bollard pull case

### Ice Milling Tests at Bollard Pull Condition

#### “Stop and Go” milling run

The purpose of this type of run was to study various details of the ice-milling, as well as to observe cavitation at various position of the ice block.

Table 4 displays the stages of the ice block approaching to the propeller and their definitions. This table can be related to a typical stop and go run as shown in Figure 11 for larger depth of cut (0.2D) and block speed of 1.5 mm/s. The numbers assigned in Table 4 are also shown in Figure 11 with reference to the block edge to propeller tip distance curve. The reader can therefore easily relate each stage of the run or position of the ice block to the propeller performance curve (i.e.  $K_T$  and  $10K_Q$ ). It is worthwhile to note that when the block to propeller tip distance is at 16mm, the block leading edge is at contact with the leading edge of the ice block.

**Table 4 Description of “Stop and Go” Milling Event**

Position	Description
1	Block approaching
2	Stop at halfway distant
3	Continue approaching
4	Block is in contact with leading edge
5	Milling
6	Propeller tip in-line with block edge
7	Continue milling
8	Stop at full stroke
9	Recess
10	Stop at halfway recess
11	Full recess

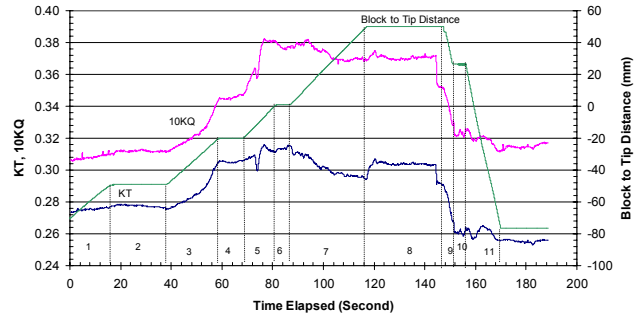


**Figure 11 Time series record at bollard condition for the “stop and go” run**

As shown in Figure 11, as the block approaches the propulsor (i.e. position 1, 2 and 3) the thrust and torque of the propeller increase, with increasing rate particularly very close to the blade (position 3). However, this increase stops when the block touches the blade leading edge (i.e. position 4). When the leading edges penetrate into the ice-block a sharp dip in the torque and thrust curve observed and this is followed by an increase in torque and decrease in thrust (i.e. position 5) until the propeller tip becomes in-line with the block leading edge (i.e. position 6). While there is virtually no change in the torque and thrust at position 6, as soon as the propeller starts milling (i.e. position 7) a considerable decrease in the thrust than in torque can be observed until the end of the milling. Once the milling stops (i.e. position 8), the thrust recovers while the torque remains more or less similar. When the propeller is operating in the ice recess at the full stroke (i.e. position 8) the thrust and torque values remain level.

#### Cavitation Observation during Milling Process

As shown in Figure 12 (position 2), when the block is at the farthest location, a slight sheet cavitation and tip vortex cavitation on the key blade at the top dead center is apparent.

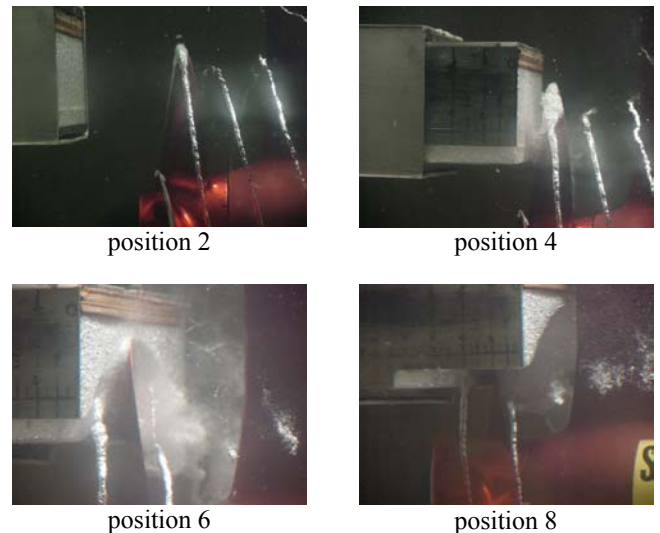


**Figure 12 Some ice-block location during ice milling test at bollard pull condition**

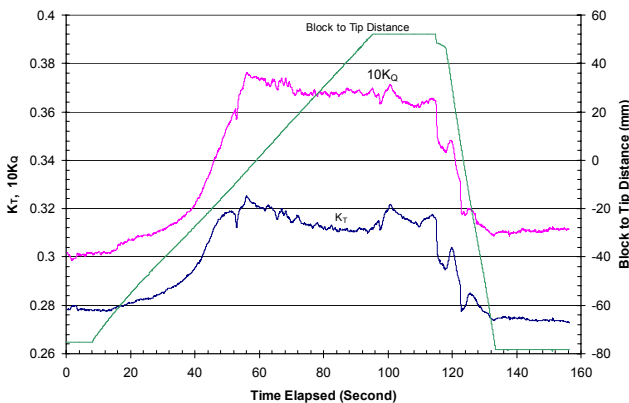
When the leading edge of the key blade is about to contact the ice-block, the sheet cavitation extends from the tip to the contact point, and the space between the frontal side of the ice block and the suction side of the key blade is filled with foam like sheet and bursting tip vortex cavitation as shown in Figure 12 (position 4)

As soon as the key blade starts the milling, the above mentioned foam like sheet cavitation transforms to severe cloud cavitation as shown in Figure 12 (position 6). While the key blade progresses, when the subsequent blade enters into the recess, the space between the suction side of the key blade and pressure side of the following blade also fills with the severe cloud cavitation. The severity of the cloud cavitation was so intense, particularly at the blade exiting side of the recess, resulting in block failure if the propeller stayed relatively long time inside the recess. Large pitting marks caused by the cloud cavitation can be easily observed inside of the milled ice blocks, particularly at the blade exiting side. This cavitation was co-existed with tremendous amount of noise.

The cloud cavitation always developed as soon as the blades entered into the recess in the above described manner even if the blade stopped milling as shown in Figure 12 (position 8). As soon as the blades come out of the recess the cloud cavitation disappears.

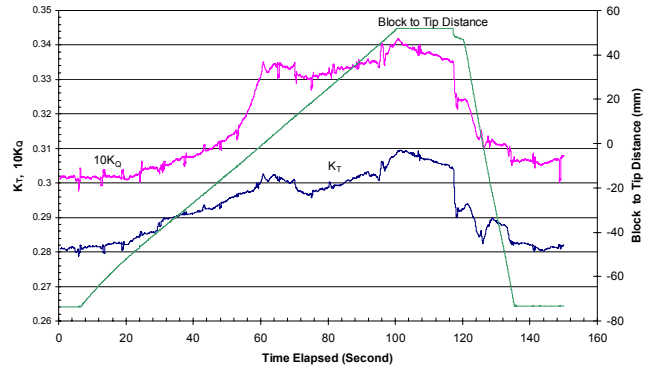
**“Continuous” milling run**

Figure 13 presents the propeller's performance and ice block position simultaneously against the elapsed time during continuous feeding of the ice block. When the block leading edge is at 16mm, the propeller touches the ice block and milling process starts. When the curve of the ice block position is flat, the model ice block is at rest. The data given in Figure 13 is for depth of cut 0.2D and 1.5 mm/s block speed.



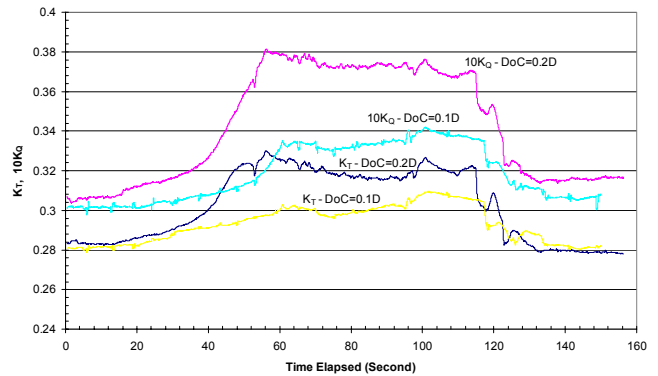
**Figure 13 Time series record at bollard condition for the continuous milling run (block Speed= 1.5 mm/s and depth of cut= 0.2D)**

In Figure 14 similar information is shown for lesser depth of cut (0.1D) but at the same block speed of 1.5 mm/s.



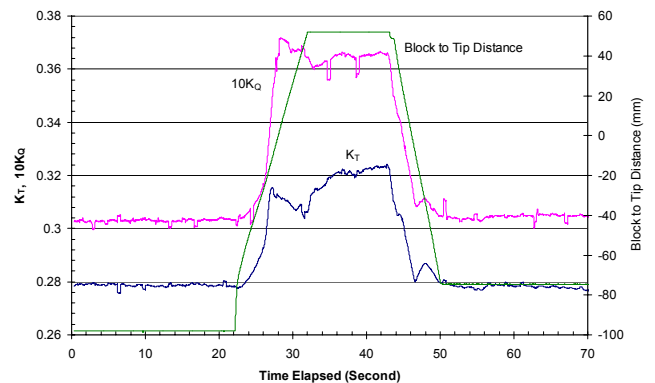
**Figure 14 Time series record at bollard condition for the continuous milling run (block Speed= 1.5 mm/s and depth of cut= 0.1D)**

Figure 15 shows the comparison of the propeller performance curve with respect to the same starting reference point at two different depth of cuts for the same block speed of 1.5 mm/s.



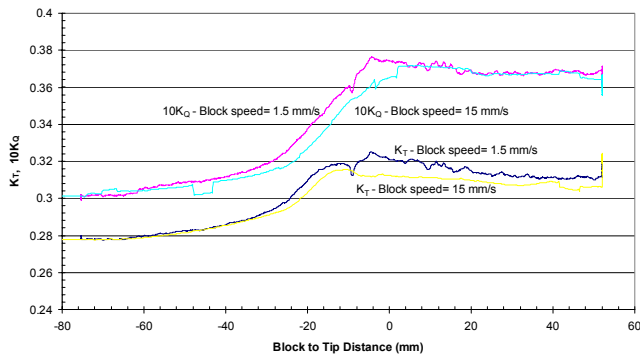
**Figure 15 Comparison between depth of cut 0.1D and 0.2D at bollard condition (block speed=1.5 mm/s)**

Figure 16 presents the simultaneous propeller performance and ice block position curves for larger depth of cut (0.2D) but 10 times as much block speed of 15 mm/s.



**Figure 16 Time series record at bollard condition for the continuous milling run (block Speed= 15 mm/s and depth of cut= 0.2D)**

Finally, Figure 17 shows the comparison of the propeller performance curves for two different block speeds plotted against the block position for larger depth of cut (i.e. 0.2D).



**Figure 17 Comparison between block speed 1.5 m/s and 15 m/s at bollard condition (depth of cut 0.2D)**

As expected, from the above figures, the change in the depth of cut results in considerable difference in the thrust and torque values measured. It appears that the larger the depth of cut the greater the effect is, as shown in Figure 15. For 0.2D depth of cut, a maximum increase of 25% in  $K_Q$  and 14% in  $K_T$  can be recorded with reference to initial  $K_T$  and  $K_Q$  values (at  $t = 0$ ), as shown in Figure 13. For 0.1D depth of cut, the increase reaches to a maximum 13% in  $K_Q$  and 9% in  $K_T$  as can be seen from Figure 14.

With regards to block speed effect, Figure 17 shows the comparison of propeller performance curves at two different block speeds (i.e. 1.5 mm/s and 15 mm/s) which indicates a slight decrease in thrust while there seems to be no difference in torque during milling. As it can be seen in Figure 16, the extent of the sharp dip during the first contact with the propeller somehow is reduced at the high-speed milling. This can be partly attributed to insufficient degree of data rate in acquisition.

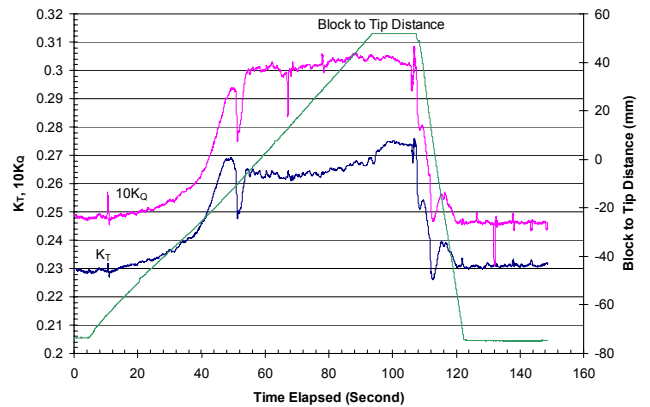
### Ice Milling test at DAT mode

In this mode, mainly continuous milling procedures were used and records of propeller performance were taken.

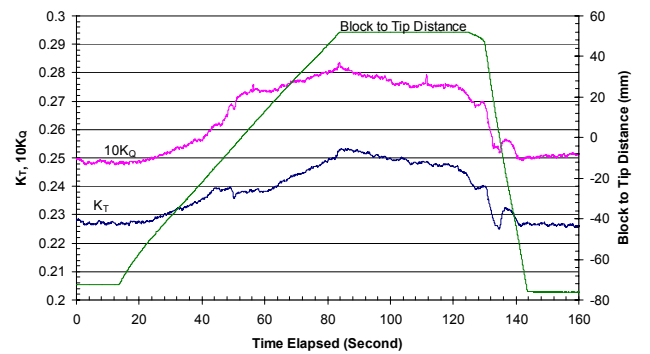
Figure 18 presents the propeller  $K_T$ ,  $10K_Q$  and ice block position plotted simultaneously against time elapsed for 0.2D depth of cut and 1.5 mm/s block speed. Similar presentation is shown in Figure 19 for 0.1D depth of cut at the same block speed.

Figure 20 shows the comparison of the above two runs with respect to same reference at the start of the runs to display effect of different depth of cut.

Figure 21 presents the results of the run performed at higher block speed with larger depth of cut.



**Figure 18 Time series record at DAT mode (block speed= 1.5 mm/s and depth of cut= 0.2D)**



**Figure 19 Time series record at DAT mode (block speed= 1.5 mm/s and depth of cut= 0.1D)**

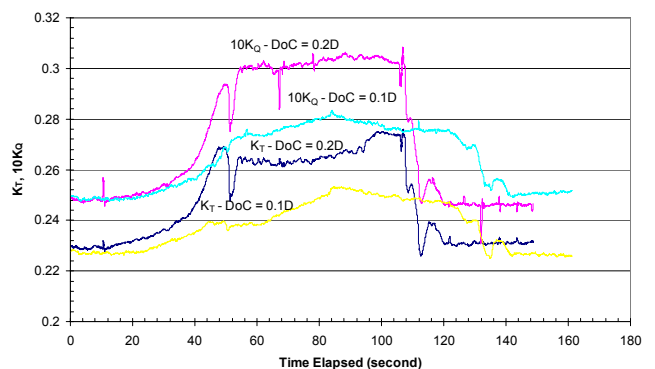


**Figure 20 Comparison between depth of cut 0.1D and 0.2D at DAT mode (block speed=1.5 mm/s)**



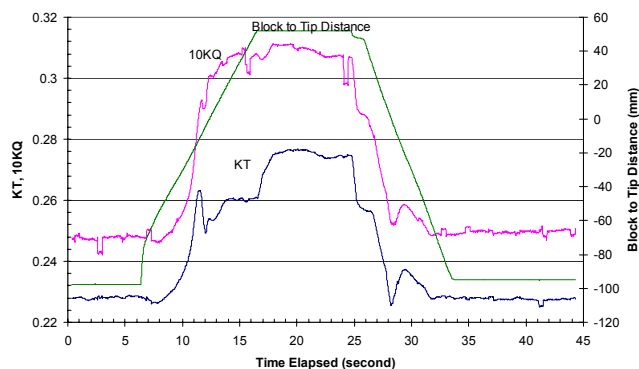


**Figure 21 Time series record at DAT mode (block Speed= 15 mm/s and depth of cut= 0.2D)**

Figure 22 compares the propeller performance curve obtained at two different block speed and 0.2D depth of cut, with respect to same reference point to demonstrate the effect of different block speed. In this figure  $K_T$  and  $10K_Q$  values are plotted against ice block distance to leading edge.

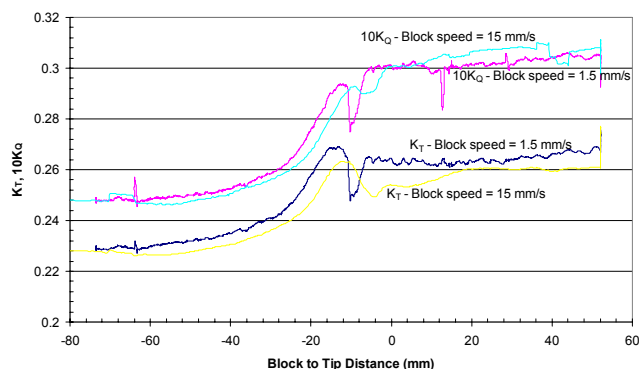


**Figure 22 Comparison between block speed 1.5 m/s and 15 m/s at DAT mode (depth of cut 0.2D)**

Test investigation in DAT mode shows that the thrust and torque characteristics exhibits similar trend to those observed in the bollard condition. However, the values are to a much lesser extent. Investigation based on Figure 18 reveals that thrust and torque also increase as the block approaches the propulsor. When the leading edge starts penetrating into the ice block, the sharp dip in thrust and torque is clearly more prominent in the DAT mode, followed by a sudden increase in their values. As soon as the propeller starts milling, thrust and torque are virtually constant until the end of milling. Similar phenomena was also found during stop milling where thrust recovers while torque remains constant

The records in DAT mode, Figure 20 shows similar trend as in the bollard condition where greater depth of cut imposes more thrust as well as torque. Figure 18 displays an increase of 22% in  $K_Q$  and 16% in  $K_T$  for 0.2D depth of cut with reference to initial  $K_T$  and  $K_Q$  at  $t = 0$ . The increase for 0.1D depth of cut is 13% in  $K_Q$  and 11% in  $K_T$  as can be seen from Figure 19.

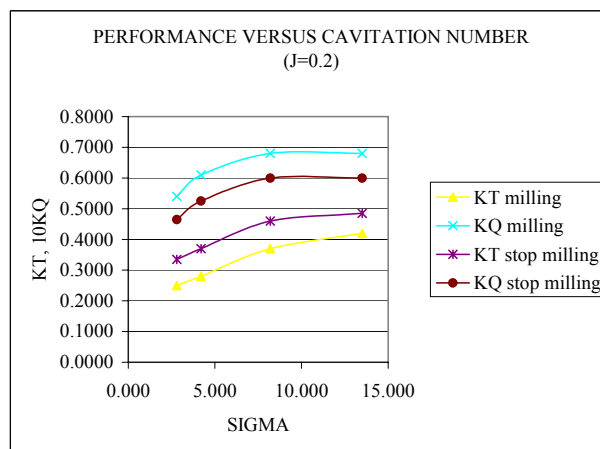
In DAT condition, similar to bollard condition, pattern of decreasing thrust with constant torque value can be shown in Figure 22 for different block speed of 1.5 mm/s and 15 mm/s.

Figure 21 also illustrates disappearing sharp dip phenomena at the first contact with the ice block, as the block speed increases.

### FURTHER REMARKS

The results presented and discussed in the previous sections regarding the cavitation observations and propeller performance in blockage and milling conditions are being reported for the first time for a podded propulsor. As stated earlier, the presence of the pod housing results in increased blade loads and hence increased cavitation, particularly in the bollard pull condition which is similar to the conditions when the vessel operating in ice-breaking (DAT) mode. The presence of the cloud cavitation and its severity in ice-milling are documented clearly with still photos and video film, as part of the investigations, in the tests.

So far, these tests have been in exploratory nature providing evidence on the cavitation phenomena and other parameters influencing the milling rather than exploring these effects systematically. Because of the time and scope of this first phase of investigations, only two loading conditions at a single cavitation number were investigated. There is a need to explore the effect of cavitation more systematically for varying cavitation numbers and at more than two loading conditions to quantify its effect on the propeller performance. Furthermore, it is also necessary to support these systematic milling tests with the blockage tests (i.e. without milling) to isolate the cavitation effect for detailed investigation including erosion tests to quantify its severity. These systematic tests are pending in the second stage of this project as part of an ongoing postgraduate study at Newcastle University in collaboration with Sumitomo.



**Figure 23 Effect of cavitation on R-Class coast guard propeller performance [11]**

Although, such systematic cavitation tests have not taken place yet with the podded propulsor, the earlier tests with R-Class Canadian coastguard propeller in the Emerson Cavitation tunnel can give some idea about the effect of cavitation as shown in Figure 23 [11]. In this figure, regardless to the cavitation number, it is clear that the milling results in approximately constant increase in torque and constant reduction in thrust for this propeller. However, when the effect of the cavitation is taken into account the difference for thrust ( $K_T$ ) and torque ( $10K_Q$ ) values over the maximum and

minimum of the cavitation number range ( $\sigma$ ) tested is 0.17 and 0.15, indicating 40% and 20% decrease, respectively. This is considerable and propeller design studies based on the performance measurements carried out in towing tanks will not take this into account beside the severe erosion effects. Whereas, assuming that the contact forces are independent of the cavitation number, one can make correction on the propeller performance ( $K_T$  and  $K_Q$ ) measured in the ice tank by performing the ice-milling tests in the cavitation tunnel.

Current practice for ice-class propeller design does not take into account the above correction. Perhaps the main factor for this is the use of large safety factor in determining the blade strength, beside the difficulty of performing such tests in cavitation tunnels. However, the performance related matters, particularly for a specialized vessel, like DAT, and its podded propulsor, will be essential to take this effect into account for more rational design procedure.

Furthermore, the cloud cavitation observed and its severity will be important from the fatigue point of view for these specialized propulsors which will have long contact periods with ice floes and ridges compared to conventional ice-breaker propellers.

## CONCLUSIONS

The paper presents, for the first time, experimental evidence and limited data on cavitation and other parameters affecting the performance of an ice-class podded propulsor in blockage and milling condition.

- From the investigations it is clear that both the torque and thrust increases during milling relative to the reference condition (i.e.  $t=0$  when the ice-block is at far away from the propulsor).
- The increase in torque during milling is partly due to mechanical contact and partly due to blockage (i.e. operating in recess) effect. The increase in thrust can only be attributed to the increased lift forces due to the blockage (i.e. operating in recess) effect since the contact with ice-block would reduce the thrust.
- The severe cloud cavitation developed during milling in recess should affect the additional thrust and torque caused by the operation in recess.
- Although the effect of cavitations is already included in the measured thrust and torque, its quantification will require further comparative tests with propeller operating in recess with/without milling at different cavitation numbers.
- The effect of cavitation should be taken into account in the design of ice-class propeller design by correcting the propeller performance data obtained in ice-tanks based on the specialised ice-milling tests in cavitation tunnels as described in this paper.

The research on this topic is being continued with further systematic tests in the Emerson Cavitation tunnel and comparison of these with ice-tank tests.

## ACKNOWLEDGMENTS

The Authors gratefully acknowledge the efforts from Mr. Ian Paterson, who is the supervisor of the Emerson Cavitation Tunnel, to set up the test rig and to perform runs in the tunnel during the project.

## REFERENCES

1. Walker, D. and Bose, N., 1994, "Hydrodynamic Loads and Dynamic Effects of Cavitation on Ice Class Propellers in Simulated Ice Blocked Flow", Proceedings of the Propeller/Shafting '94 Symposium, SNAME, pp. 20-1 to 20-19.
2. Doucet, J.M., Bose, N., Walker, D. and Jones, S.J., 1995, "Cavitation Erosion on a Model Ice Class Propeller in Blocked Flow", PROPCAV'95, Newcastle upon Tyne, 16-18 May, pp. 229-238.
3. Mintchev, D., Bose, N., Atlar, M., and Paterson, I., 1999, "Propeller Ice Milling Tests in a Cavitation Tunnel, Report No. MT-1999-10, Department of Marine Technology University of Newcastle and Report No. OERC-1999-002 Ocean Engineering Research Centre-Memorial University of Newfoundland.
4. Mintchev, D., Bose, N., Veitch, B., Atlar, M., Paterson, 2000. Propeller Ice Milling Tests in the Emerson Cavitation Tunnel, NCT50, Newcastle upon Tyne, England, 3-5 April, pp.315-326.
5. Backlund, A. and Matsuda, M., 2000, "New Ship Concepts with Azipod Propulsion", Ship Propulsion Systems, Intl multi-stream Conference, Manchester, 4-5 December.
6. Sasaki, N., Laapio, J., Fagerstrom, B. and Juurma, K., 2001, "Model Tests of Ice Going Duple Acting Aframax Tanker", Proceedings of 6<sup>th</sup> Canadian Marine Hydrodynamics and Structures Conference, Vancouver.
7. Aryawan, W.D., Prasetyawan, I., Atlar, M., Wang, D., Paterson, I., 2000, "Open Water Cavitation Tunnel Tests for Propeller Model No. P446 With and Without Pod", Report No. MT2002-030, Emerson Cavitation Tunnel – University of Newcastle.
8. Atlar, M., Prasetyawan I., Aryawan W.D., Wang D. Paterson I., 2002, "Ice Milling Tests with a Model Podded Propulsor", Report No. MT2002-031, Emerson Cavitation Tunnel – University of Newcastle
9. Atlar, M., 2000, "A History of The Emerson Cavitation Tunnel and Its Role in Propeller Cavitation Research", International Conference on Propeller Cavitation NCT50-April 2000, Newcastle upon Tyne, U.K.
10. Leathard, F.I., 1985, "Emerson Cavitation Tunnel Operating Instruction", Report No. 1/85, Emerson Cavitation Tunnel – University of Newcastle.
11. Mintchev, D., Bose N., Veitch, B., Atlar, M. and Paterson, 2001, "Some Analyses of Propeller Ice Milling Tests", Proceedings of 6<sup>th</sup> Canadian Marine Hydrodynamics and Structures Conference, Vancouver.